ANALYSIS OF UNKNOWN VELOCITY AND TARGET OFF THE GRID PROBLEMS IN COMPRESSIVE SENSING BASED SUBSURFACE IMAGING

Ali Cafer Gurbuz

Dept. of Electrical and Electronics Eng., TOBB University of Economics and Technology
Sogutozu Cad No: 43, 06560, Ankara, Turkey
phone: + (90) 3122924323, email: acgurbuz@etu.edu.tr

ABSTRACT

Sparsity of target space in subsurface imaging problem is used within the framework of the compressive sensing (CS) theory in recent publications to decrease the data acquisition load in practical systems. The developed CS based imaging methods are based on two important assumptions; namely, that the speed of propagation in the medium is known and that potential targets are point like targets positioned at discrete spatial points. However, in most subsurface imaging problems these assumptions are not always valid. The propagation velocity may only be known approximately, and targets will generally not fall on the grid exactly. In this work, the performance of the CS based subsurface imaging methods are analyzed for the above defined problems and possible solutions are discussed.

1. INTRODUCTION

In recent years the sparsity information about the signals has found itself a variety of very interesting applications including image reconstruction [1], medical imaging [2], radar imaging [3], shape detection [4] and direction of arrival estimation [5]. In these applications the sparsity information about the signals led to lower number of measurements for correct reconstruction. The recent theory of compressive sensing (CS) [6–8] details the reconstruction of sparsely representable signals from very small number of linear measurements. Assume a K-sparse signal $x = \Psi s$ with length N, where x is sparse in the basis Ψ with at most K nonzero entries in s. Instead of measuring all N componenets of x, CS takes small number of M non-traditional linear measurements in the form of $y = \Phi x$. The signal x can be reconstructed exactly from $M = C\left(\mu^2(\Phi,\Psi)\log N\right)K$ [9] compressive measurement with high probability by solving a convex optimization problem of the following form:

$$\min \|s\|_1, \qquad \text{subject to} \quad y = \Phi\Psi s \tag{1}$$

which can be solved efficiently with linear programming. The optimization program in (1) selects the sparsest signal constraint to the measurements y. The required number of measurements are only on the order of $O(K\log(N))$.

Although CS enables lower required data acquisition, it is more important in areas where data acquisition is hard or expensive. One such area is remote sensing and radar imaging. CS theory is first used in radar literature in [3] where in simulation it was demonstrated that the radar profile could be constructed with less number of measurements. Later in [10, 11] the compressive sensing ideas are extended to time domain and stepped frequency ground penetrating radar (GPR) for subsurface imaging with experimentally shown results. In the development of the theory, the target space was discritized and assumed to be composed of small number of point reflectors. A linear relationship (transform or dictionary) between the discritized target space and the measured time domain samples are constructed assuming a known velocity of propagation in the subsurface medium. Instead of measuring frequency steps, it was shown that much cleaner (sparser), robust and high resolution images could be obtained using small number of random frequency step measurements resulting a practical decrease in total data acquisition time. Recently extended works about MIMO radar [12] and CS based remote sensing [13] have also been published.

The developed CS based subsurface imaging methods [10, 11] create a model GPR data dictionary by first discritizing the target space and synthesizing the model GPR data for each discrete target space position for the data acquisition process of the radar. Later the imaging problems are formalized as representing the data from the created overcomplete dictionary. However there are two important points needing further exploration. First the actual targets might not be point targets exactly on the grid positions. Depending on the discritization density actual points will be off the grid with varying levels of distance. It is important to understand the effect of the grid and the grid size on the imaging performance. The second problem is to create the model GPR data. This requires the knowledge of the wave propagation velocity in the subsurface. Although this could be estimated or known approximately in practice it is usually not known priori, thus it is important to understand the effect of mismatch between the true and assumed velocities on the imaging performance. This paper analyzes these two problems and discusses possible solutions.

In Section 2 the CS based subsurface imaging method is briefly summarized since the later sections uses and refers to those results. Velocity mismatch problem is analyzed in Section 3 and the griding problem is discussed in Section 4. Conclusions are drawn in Section 6.

2. CS BASED SUBSURFACE IMAGING

The standard backprojection algorithms [14] generate subsurface images by mainly applying a matched filter of the measured data with the impulse response of the data acquisition process. Different from the backprojection methods, the goal in CS based subsurface imaging is to represent the measured data as a linear combination of possible measurements from a dictionary. By this way any possible prior information like sparsity could be used. Hence a GPR data dictionary should be constructed.

A stepped frequency GPR (SF-GPR) is considered. A detailed explanation on CS based imaging about SF-GPRs is

 ISSN 2076-1465

given in [11]. Here only a summary is presented for this paper. To generate a dictionary for GPR data, a target model for which the expected target return can be calculated should be selected. Although not required a simple point target model is selected since the response from a point target can easily be modeled. In addition to this, the total target space can be seen as combination of small number of point targets making the sparsity assumption feasible. Assume an SF-GPR taking measurements over P targets. The received frequency measurements at the i^{th} scan point can be written as

$$d_i = \sum_{k=1}^{P} r_k e^{-j\omega(t-\tau_i(p_k))} \tag{2}$$

where $\tau_i(p_k)$ is the time delay for the target at the position p_k and when the antenna is at the i^{th} scan position. Note that for correct calculation of the time delay from each GPR position to each target position requires the knowledge of the wave propagation velocity in the medium. Target reflectivity or other effects are combined in the weights r_k. To represent the i^{th} scan data d_i as a linear combination from a data dictionary the target space π_T is discritized to generate a finite set of target points $T_S = \pi_1, \pi_2, ..., \pi_N$ where N determines the total number of possible discrete target space points and each π_j is a 3D vector $[x_j, y_j, z_j]$ representing one possible target space point. A GPR data dictionary can be generated by synthesizing the time/frequency data for each possible target space point π_j. Hence when the GPR is at the i^{th} scan point the j^{th} column of the dictionary, corresponding to a target at π_j can be written as

$$[\Psi_i]_j = \exp[-j\omega(t-\tau_i(\pi_j))] \tag{3}$$

Repeating (3) for each discrete possible target position creates the dictionary Ψ_i. This is the dictionary for only the i^{th} scan position. Note that the dimension of Ψ_i will be $L \times N$ if L frequency steps are used. Depending on the discritization level, N, the possible target points π_j will be close to the actual target points p_k. Hence the measured data d_i can be represented as a linear combination of the dictionary columns $[\Psi_i]_j$ as

$$d_i = \Psi_i b + e \tag{4}$$

where b is a weighted indicator vector defining the target space and e representing any unmodelled factor or noise. From the linear relation defined in (4) the goal is to find b which is actually an image of the medium.

Standard SF-GPRs measure a regularly spaced set of L frequencies in the frequency band they are using. Sparsity of the target space leads to less number of measurements, thus instead of measuring L frequencies only a small random subset, M of them are measured at each scan point. Here $M < L$. The taken measurements are $\beta_i = \Phi_i d_i$ where Φ_i is designed to be an $M \times L$ measurement matrix constructed by randomly selecting M rows of an $L \times L$ identity matrix. This effectively reduces the data acquisition time of the SF-GPR by L/M. Using measurements β_i from S different scan positions the target space b is constructed [15, 16] by solving

$$\hat{b} = \arg\min \|b\|_1 \qquad \text{s.t.} \quad \|A^T(\beta - Ab)\|_\infty < \varepsilon \tag{5}$$

where $\beta = [\beta_1^T, \ldots, \beta_S^T]^T$, $\Psi = [\Psi_1^T, \ldots, \Psi_S^T]^T$, $\Phi = \text{diag}\{\Phi_1, \ldots, \Phi_S\}$ and $A = \Phi\Psi$

3. VELOCITY MISMATCH PROBLEM

One of the most important problems in the method summarized in Section 2 is that the true propagation velocity might be different than the velocity assumed for the creation of the dictionary in 3. It is important to understand the effect of this velocity mismatch on the CS imaging performance. To do so, a simulated GPR data set from a single point target at $(x, z) = (0, -8)$ cm is generated using a true propagation velocity of $v = 2 \times 10^{10}$ cm/s. The test data is used to image the target space with assumed velocities varying from 1×10^{10} cm/s to 3×10^{10} cm/s. Hence dictionaries are created with the assumed velocities. For each assumed velocity 100 independent images are computed with different noise realizations with signal to noise ratio (SNR) equals 10 dB and with different random measurement matrices at each trial. Figure 1 shows the mean images out of these 100 trails.

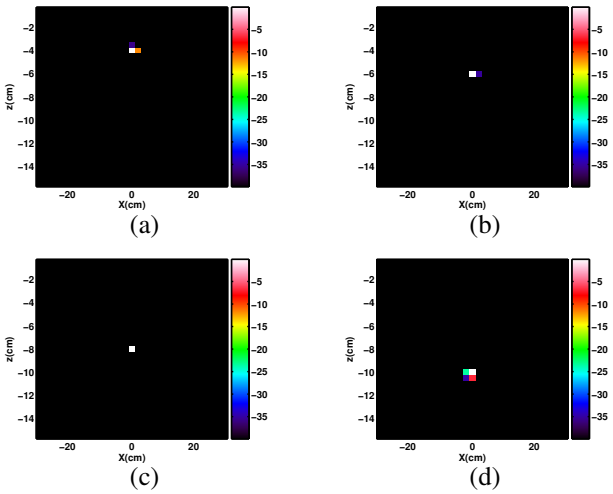

Figure 1: Average of the 100 independent imaging assuming the propagation velocity is (a) 1×10^{10} cm/s, (b) 1.5×10^{10} cm/s, (c) 2×10^{10} cm/s, (d) 2.5×10^{10} cm/s.

Note that the actual target is at one of the grid positions exactly and when there is no velocity mismatch, i.e., assumed velocity is same as the true velocity 2×10^{10} cm/s, the single target is correctly found at its true position. Interestingly when there is even important amount of velocity mismatch the CS based imaging could still generate focused images but the target appears at incorrect depths. This is because first the CS based imaging algorithm tries generate sparse results and second the dictionary model data for a different target position is similar to the measured data from a different position and velocity. The average distance of the estimated target point from the true target position is shown in Fig. 2 as a function of the assumed velocity.

When the assumed velocity is the same as the true velocity for the medium the target is imaged as a single point at its correct position as shown in Fig. 1(c). The distance of the estimated target position from the correct target position increases as the assumed velocity is further from the true velocity of the medium. It is important to note that the CS method locates the x axis of the target correctly while the unknown velocity affects the depth estimate only. The

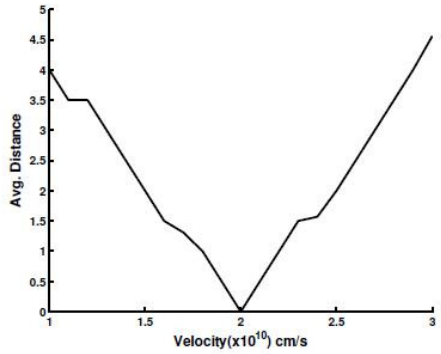

Figure 2: Distance of the estimated target point from the true target location as a function of the assumed velocity

reason for this depth shift again is that the optimization in (5) matches the measured data best with the given constraint using a dictionary element corresponding to a target at another depth. To see this better, Fig. 3(a) shows the model GPR data from a target at $(x,z) = (0,-8)$ using $v = 2\times 10^{10}$ cm/s, while Fig. 3(b) shows the model GPR data from a target at $(x,z) = (0,-4)$ using $v = 1\times 10^{10}$ cm/s. The similarity of these dictionary elements in two different dictionaries explains the results in Fig.1.

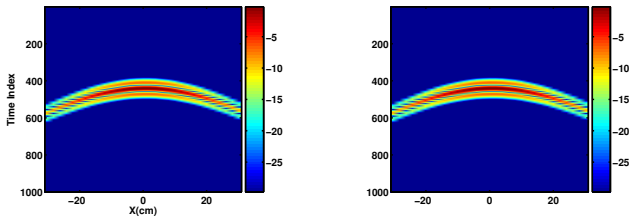

(a) (b)

Figure 3: Model GPR data (a) for a target at $(x,z) = (0,-8)$ using $v = 2\times 10^{10}$ cm/s and (b) for a target at $(x,z) = (0,-4)$ using $v = 1\times 10^{10}$ cm/s.

To determine the amount of depth shift consider a single homogeneous medium where targets and antenna are both in the same medium as shown in Fig. 4.

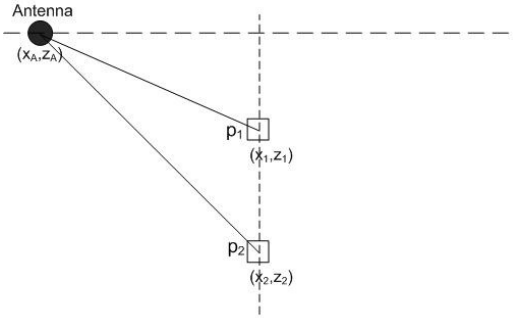

Figure 4: Two point targets in a homogeneous medium

The total time delay for two points targets p_1 and p_2 shown in Fig. 4 are $\tau_1 = \frac{2\sqrt{(x_A-x_1)^2+(z_A-z_1)^2}}{v_1}$ and $\tau_2 = \frac{2\sqrt{(x_A-x_2)^2+(z_A-z_2)^2}}{v_2}$ respectively. It can be noted that if $x_1 = x_2$ then it is possible to get $\tau_1 = \tau_2$ for all antenna positions (throughout the full scan) if $|z_A - z_2| = \frac{v_2}{v_1}|z_A - z_1|$. This means that if the target space was homogeneous, applying our method with an unknown velocity v_2 that is different from the true velocity v_1 will result a target space image with only p_2 instead of the correct target position p_1, since the measured data can be exactly matched using the element of the data dictionary corresponding to p_2. Since the results in Fig. 1 are from a 2-layer medium (air and soil), we dont observe this exact representation ; but similarly we observe focused images with sparsely selected target points.

Although there might be exactly represented data for different velocities for a single homogeneous medium, extended dictionaries can be used to both create a target space image and estimate the wave propagation velocity. For the extended dictionary case a combined dictionary is created using a discrete set of varying possible medium velocities and the imaging problem defined in (5) is solved to obtain the target image. Using V number of discrete velocities extends the dictionary V times, thus the obtained vector b is of length VN where each length N part corresponds to the image with the corresponding assumed velocity. A simulation is presented next detailing the extended dictionary idea for the unknown velocity problem. Assume the target space with 3 point reflectors at the corresponding positions as shown in Fig. 5(a). The space is 40×40 cm^2 area in x-z dimensions discritized with 2 cm grid size resulting a total of 400 discrete target space points. Actual targets are assumed to be on the grid points and the true wave propagation is assumed to be $v = 2\times 10^{10}$ cm/s. A bistatic antenna with antenna height of 10 cm and transmitter-receiver distance of 5 cm takes step frequency measurements above the ground. The medium velocity is assumed unknown and an extended GPR data model dictionary is created for velocities $1.8, 1.9, 2, 2.1, 2.2\times 10^{10}$ cm/s, thus the extended dictionary is 5 times wider than the standard dictionary used in CS based method. When the imaging is done with the explained extended dictionary, the images corresponding to each velocity case is shown in Fig. 5. The created images are normalized to the maximum of them all and they are all shown in the same 30dB scale.

As seen from Fig.5 although nothing is assumed about the medium velocity the 3 target points appear only in the image corresponding to the true velocity of the medium. In 30dB scale no other targets are visible in other velocity images. This shows that extended dictionary can be used to create radar images where the wave propagation is not known exactly but estimated in a range of velocities. Although preleminary results shown in Fig.5 indicate promising conclusions, still important amount of research should be done to understand pros and cons of such a method in varying conditions. First using extended dictionaries increases both the memory and computational requirements of CS based imaging methods. Sub optimal greedy based methods [17] could be used together with extended dictionaries. Next robustness of such a method to small variations in velocity and the noise level should be analyzed. Direct velocity estimation algorithms from compressed measurements could also be developed.

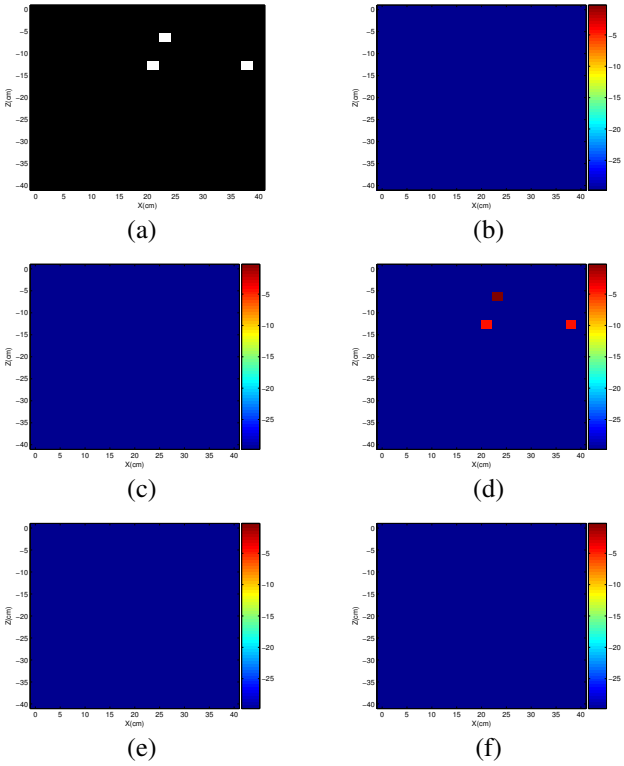

Figure 5: (a) Correct target space image, Target space image corresponding to the dictionary part for the velocity (b) $v = 1.8e+10$ cm/s, (c) $v = 1.9e+10$ cm/s , (d) $v = 2e+10$ cm/s, (e) $v = 2.1e+10$ cm/s, and (e) $v = 2.2e+10$ cm/s

4. TARGET OFF THE GRID PROBLEM

Another problem in dictionary selection algorithms is that the actual targets don't correspond exactly to any of the grid positions thus the columns of the dictionary don't exactly represent the measured data. In this part velocity of the medium is assumed known and the effect of the grid size on the created subsurface images is analyzed only. A target space imaged with a grid size of 1 cm in both x and z dimensions and with 30×30 cm^2 area is simulated. The target space consists 3 point reflectors at off the grid positions as (7.3,-12.6), (21.34,-8.9), and (16.5,-22.5). An SNR of 10dB is used. The image obtained from the simulated data is shown in Fig.6(a). Although the targets are not exactly on the grid positions, the imaging algorithm could locate the targets. The reason for this is that the discritization is fine enough so that the optimization algorithm could match the data within the relaxed constraint using the corresponding closest dictionary columns. The correct positions of the targets are marked with circles on the images. Next the discritization in the target space is increased to 2 cm in both x and z dimensions. The same data is used to create the target space with this increased grid size. The obtained image is shown in Fig.6(b). Since each dictionary column corresponds to possibly more distant target space points, it is harder to match the measured data using the dictionary. However for the grid size of 2 cm still the targets could be located correctly but the sparsity of the target space is less.

When the grid size is 3 cm the 3 peaks in the created

Figure 6: Imaging for the targets off the grid with grid size (a) 1cm, (b) 2cm, (c) 3cm, (d) 5cm

image close to the correct target positions can still be seen although small variations all over the image start to increase. Further increasing grid size to 5 cm creates totally a wrong target space image. One advantage of higher grid size is that the computational complexity of the algorithm decreases since the total number of discrete points, N, decreases. Also it can be seen that the discritization creates no problems until a threshold grid size. This point can also be viewed as the possibility of a multiresolution imaging. The target space image can be created using a rough discritization which would be around 3 cm for this case and the selected target areas can be imaged using a finer grid in iterative steps. The future work in this area will focus on understanding the relation between the used GPR system and transmitted pulses with the data constraint parameter ε in (5) and the maximum allowable grid size for correct target space reconstruction.

5. ACKNOWLEDGEMENTS

This work was partially supported by The Scientific and Technical Research Council of Turkey (TUBITAK) under contract agreement 109E280 and within the Marie Curie IRG Grant with grant agreement PIRG04-GA-2008-239506.

6. CONCLUSIONS

In this paper the two important assumptions; namely, that the speed of propagation in the medium is known and that potential targets are point like targets positioned at discrete spatial points are analyzed for the compressive sensing based imaging algorithms. In most subsurface imaging problems these assumptions are not always valid. It was shown that an extended dictionary can be used covering a range of possible medium velocities can be used to both create a correct target space and a velocity estimate. Also it was shown that the off the grid targets could be successfully imaged until the grid size is below some threshold leading to the possibility of multiresolution imaging. Also it should be noted that all these problems are worked under the low number of measurement case compared to standard backprojection algorithms.

REFERENCES

[1] D. Takhar, J. N. Laska, M. B. Wakin, M. F. Duarte, D. Baron, S. Sarvotham, K. F. Kelly, and R. G. Baraniuk, "A new compressive imaging camera architecture using optical-domain compression," in *Proc. Comp. Imaging IV at SPIE Electronic Imaging*, 2006.

[2] M. Lustig, D. Donoho, and J. Pauly, "Sparse MRI: The application of compressed sensing for rapid MR imaging," *Magnetic Resonance in Medicine*, vol. 58, no. 6, pp. 1182–1195, Dec. 2007.

[3] R. Baraniuk and P. Steeghs, "Compressive radar imaging," in *IEEE Radar Conf.*, 2007, pp. 128–133.

[4] N. Aggarwal and W. C. Karl, "Line detection in images through Regularized Hough Transform," *IEEE Trans. on Image Processing*, vol. 15, pp. 582–590, 2006.

[5] A. C. Gurbuz, V. Cevher, and J. H. McClellan, "A compressive beamformer," in *ICASSP 2008*, Las Vegas, Nevada, March 30 –April 4 2008.

[6] D. Donoho, "Compressed sensing," *IEEE Trans. Information Theory*, vol. 52, no. 4, pp. 1289–1306, 2006.

[7] E. Candes, J. Romberg, and T. Tao, "Robust uncertainty principles: Exact signal reconstruction from highly incomplete frequency information," *IEEE Trans. Information Theory*, vol. 52, pp. 489–509, 2006.

[8] R. Baraniuk, "Compressive sensing," *IEEE Signal Processing Magazine*, vol. 24, no. 4, pp. 118–121, July 2007.

[9] E. Candes and J. Romberg, "Sparsity and incoherence in compressive sampling," *Inverse Problems*, vol. 23, pp. 969–985, 2006.

[10] A. C. Gurbuz, J. H. McClellan, and W. R. Scott Jr., "Compressive sensing for subsurface imaging using ground penetrating radars," *Signal Processing*, vol. 89, no. 10, pp. 1959–1972, 2009.

[11] A. C. Gurbuz, J. H. McClellan, and W. R. Scott Jr., "A compressive sensing data acquisition and imaging method for stepped frequency gprs," *IEEE Trans. Signal Processing*, vol. 57, no. 7, pp. 2640–2650, 2009.

[12] Y.Yu, A. Petropulu, and H. Poor, "Compressive sensing for mimo radar," in *ICASSP*, 2009, pp. 3017–3020.

[13] A. C. Fannjiang, P. Yan, and T. Strohmer, "Compressed remote sensing of sparse objects," in *Archieve*, 2009.

[14] D. Daniels, *Ground Penetrating Radar, 2nd Ed.* The Institution of Electrical Engineers (IEE), 2004.

[15] E. Candès, J. Romberg, and T. Tao, "Stable signal recovery from incomplete and inaccurate measurements," *Comm. on Pure and Applied Math.*, vol. 59, no. 8, pp. 1207–1223, 2006.

[16] D. Donoho, M. Elad, and V. Temlyakov, "Stable recovery of sparse overcomplete representations in the presence of noise," *IEEE Trans. Information Theory*, vol. 52, no. 1, pp. 6–18, 2006.

[17] J. Tropp and A. Gilbert, "Signal recovery from random measurements via orthogonal matching pursuit," *IEEE Trans. Information Theory*, vol. 53, no. 12, pp. 4655–4666, Dec. 2007.